

Reflection control in hyper-NA immersion lithography

Zhimin Zhu^a, Emil Piscani^b, Kevin Edwards^a, Brian Smith^a

^aBrewer Science, Inc., 2401 Brewer Drive, Rolla, Missouri 65401, USA

^bResist Test Center, International SEMATECH, 255 Fuller Road, Albany, New York 12203, USA

ABSTRACT

The impact of bottom reflection on critical dimension (CD) processing window is intensively investigated with a simulation using a full diffraction model (FDM) in which the effective reflectivity is calculated from standing wave amplitude. Most importantly, the optical phase shift of the reflection is used as a design criterion and was found to be the primary factor that affects the UV distribution, and, hence, has a strong impact on exposure latitude and depth of focus. Foot exposure (FE) is introduced as a new metric to characterize the phase shift. Some single-layer and dual-layer bottom anti-reflective coating (BARC) designs were implemented with an Exitech MS-193i immersion micro-stepper (NA=1.3) for 45-nm dense lines at the Resist Test Center (RTC) at International SEMATECH, Albany, New York. The experimental results show that FE is closely related to the CD processing window. In contrast to conventional BARC usage, a small amount of substrate reflection with a controlled optical phase shift dramatically improves CD processing window.

Key words: immersion; optical phase shift, foot exposure (FE), effective reflectivity, full diffraction model (FDM), CD processing window

1. INTRODUCTION

Conventional bottom anti-reflective coating (BARC) techniques have been used to eliminate UV standing waves in photoresist layers.^[1] When exposure wavelengths are reduced to 193 nm and the feature sizes in integrated circuits are continuously pushed to less than 65 nm, the lithography process actually has higher tolerance to UV standing waves due to photoacid diffusion. In some cases, the sidewall of a line profile is straight even though the simulated UV standing wave amplitude is as high as 67%, based on an effective reflectivity of 2.5%. Eventually, substrate reflection totally changes the UV distribution in the resist, and our experiments also demonstrate its great impact on the processing window of critical dimension (CD). Conventional BARC design considers only scalar reflectivity and ignores the optical phase shift that primarily determines UV distribution. Therefore, the simulated reflectivity does not correlate to lithography performance. In practice, a manufacturer chooses BARC layer thickness from experimental optimization, and usually the optimum thickness deviates from what the simulation proposed. Foot exposure (FE) is introduced in this work as a new metric to characterize the optical phase shift of substrate reflection to determine UV distribution. It turns out that FE is more correlated to CD window than scalar reflectivity. Another useful function of FE is to diagnose material footing or undercut problems.

2. SIMULATION APPROACHES

Conventional BARC simulation works on incident angle or Fourier domain. It collects the reflectivity from all illumination angles and diffraction angles, and then gives a single value for overall reflectivity. One inconsistency that often arises is that the reflection from different diffraction angles is collected in an incoherent manner while lithography imaging is a coherent process. A second inconsistency is that for incoherent illumination the standing waves from different incident angles are shifted with respect to each other in the vertical direction, resulting in a smoothed standing wave. Thus, for a given overall reflectivity value, the standing wave amplitude depends also on the coherency of the illumination source, and it is unreasonable to set a reflectivity criterion for every possible optical setup. A third inconsistency is that a single reflectivity value does not contain the pattern-related details of the reflectivity. The reflectivity should be pattern dependent and distributed in the aerial image plain.

Optical Microlithography XXI, edited by Harry J. Levinson, Mircea V. Dusa,
Proc. of SPIE Vol. 6924, 69244A, (2008) · 0277-786X/08/\$18 · doi: 10.1117/12.772899

Z. Zhu, E. Piscani, K. Edwards, B. Smith, "Reflection control in hyper-NA immersion lithography," *Proceedings of SPIE*, vol. 6924, 6924-163, 2008. □
Copyright 2008 Society of Photo-Optical Instrumentation Engineers. One print or electronic copy may be made for personal use only. Systematic reproduction and distribution, duplication of any material in this paper for a fee or for commercial purposes, or modification of the content of the paper are prohibited.

The simulation tool described here works on both Fourier and aerial image planes. For one illumination angle (or one illumination sigma point), the aerial image is obtained from the interference of forward and reflected images, and then the UV distribution is obtained from the accumulation of the images from all illumination angles. Finally the resulting effective reflectivity is calculated from the standing wave amplitude of the UV distribution. In terms of standing wave control, the reflectivity criterion is independent of the optical setup. The distribution of the reflectivity in the aerial image plane depends on the mask pattern. Therefore pitch dependence can be analyzed within a mask. Effective reflectivity is evaluated in a photoacid diffusion region around line edges, ignoring the standing waves in an open area. In comparison to a commercial tool, this new tool gives the exact same results as PROLITH™ simulation when both are used to simulate an interferometer scanner. The new tool also agrees with SOLID E simulation if the mask is a single pitch grating. For general cases, the present simulation tool gives more logical results than either of these alternative packages.

The effective reflectivity is only one way to predict standing wave amplitude, but a new concept from this work, defined as foot exposure (FE), provides better insight to characterize the optical phase shift of reflectivity to differentiate UV distributions. FE is the ratio of UV intensities near the resist bottom (averaged in a diffusion region) to the average intensity at the line edge. FE is closely related to the optical phase shift of the reflectivity. When the phase is varying, the standing wave shifts along the vertical direction, and FE swings accordingly. If FE equals 1, the bottom region receives average exposure. Normally FE should be a little bit greater than 1 to compensate for photoacid loss due to diffusion into the BARC layer or substrate. The choice of FE also depends on BARC material modifications. An individual BARC material may contain a photoacid generator (PAG) and contribute a certain acid level independent of the resist.

3. EXPERIMENT

The lithography tool is an Exitech MS-193i immersion microstepper with a 1.30 NA 20X reduction projection optical system. On-axis illumination aperture $0.82\sigma_c:0.15\sigma_r$ is chosen to print 45-nm 1:1 patterns. XY polarization is applied to have high image contrast. The stack is shown in Figure 1. Brewer Science, Inc., product ARC®100 with $n=1.67$ is used throughout this investigation. The extinction coefficient k is available continuously in the range from 0.13 to 0.47. One advantage of this material is high etch rate. The thickness of the BARC layer was precisely measured.

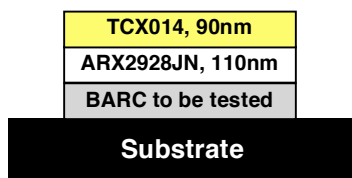


Figure 1. JSR ARX2928 photoresist is used for the experiment. The top coat TCX014 was used to prevent resist leaching into the immersion water.

Single-layer BARC on silicon substrate

The simulation results are shown in Figure 2(a). The solid curve is the effective reflectivity, and the dotted curve is FE. Three thickness points on the curves around the first minimum reflectivity are taken for lithography testing. Figure 2(b) is the UV distribution in the resist across the line pattern and along the vertical direction. The peaks of the standing wave are shifted from each other depending on the optical phase shift. For the left point the peak is located at bottom so that it presents a high FE value. The right point has very low FE because the peak of the standing wave is far above bottom. Figures 2(c) and (d) show the CD measurement at the middle of line profile height. The measurement is taken for different exposure doses and depths of focus. The greater the number of measurable data points and the closer they gather along the y-axis direction, the wider the CD processing window. From these results, a preliminary conclusion can be made that minimum reflectivity does not give the widest process window. A wide processing window occurs when there is enough FE level even though the effective reflectivity is as high as 2.5%, which is equivalent to approximately 4% of total reflectivity from conventional simulation. Figure 2(f) also indicates that low FE causes footing problems.

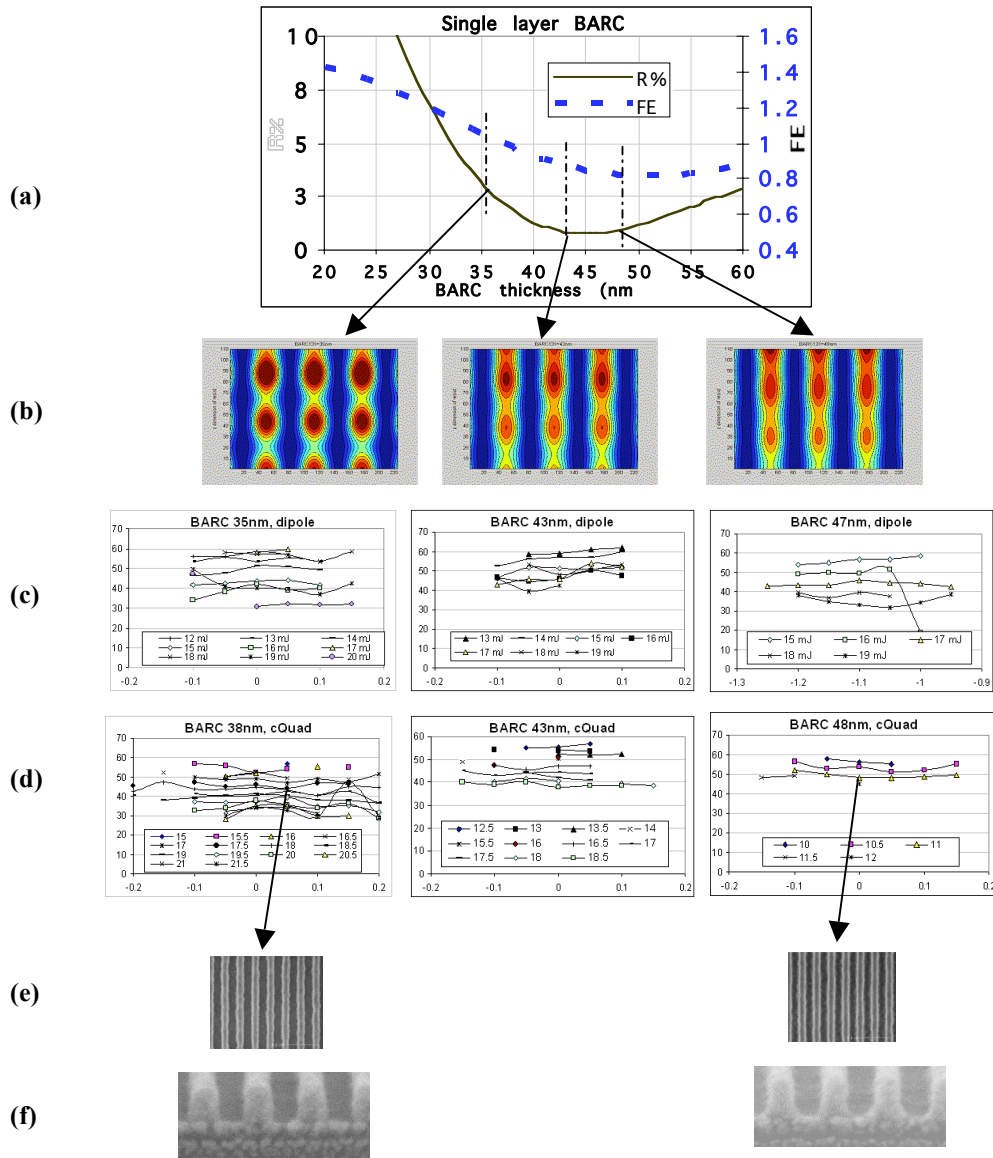


Figure 2. Single-layer BARC simulation and experimental results; (a) effective reflectivity; (b) UV distribution in resist; (c) measured CD size at line waist versus depth of focus at different exposure doses for dipole illumination, where y-axis is CD size in nm and x-axis is depth of focus in microns; (d) CD measurement for on-axis quadrupole illumination; (e) top-down CD SEM picture; (f) cross-section SEM picture.

Dual-layer BARC on a silicon substrate

A dual-layer BARC system adds three more dimensions of reflection control and potentially gives better lithography performance. ARC[®]145 and ARC[®]113 materials are used as the upper and lower BARC materials with k values of 0.45 and 0.13, respectively. Figure 3(a) is the contour map of effective reflectivity with respect to upper and lower BARC layer thicknesses, and (b) is the map for FE. Sixteen points of different thickness combinations were tested, as indicated by white dots in the map. This experiment design presents very good statistical confidence in terms of the number of different stacks and the number of CD measurement data points.

Figure 4 gives the test results of the 16 points except for the first point. This point has high reflectivity and low FE; the CD profile is too poor to be measured. From Figure 4, low reflectivity regions do not give good performance while the preferred FE region has a much wider CD processing window.

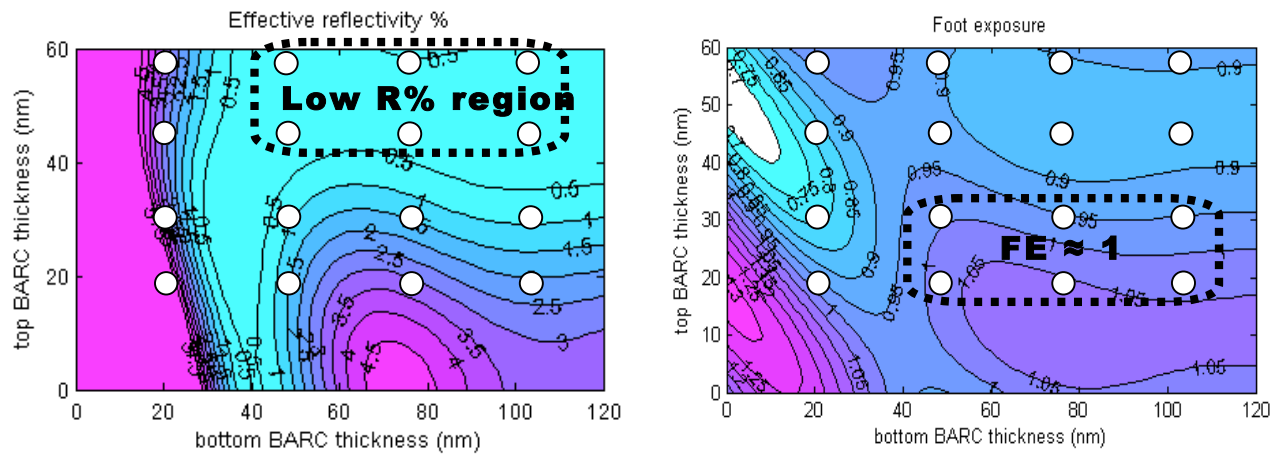


Figure 3. Dual-layer BARC simulation results: (a) contour map of effective reflectivity; (b) contour map of foot exposure.

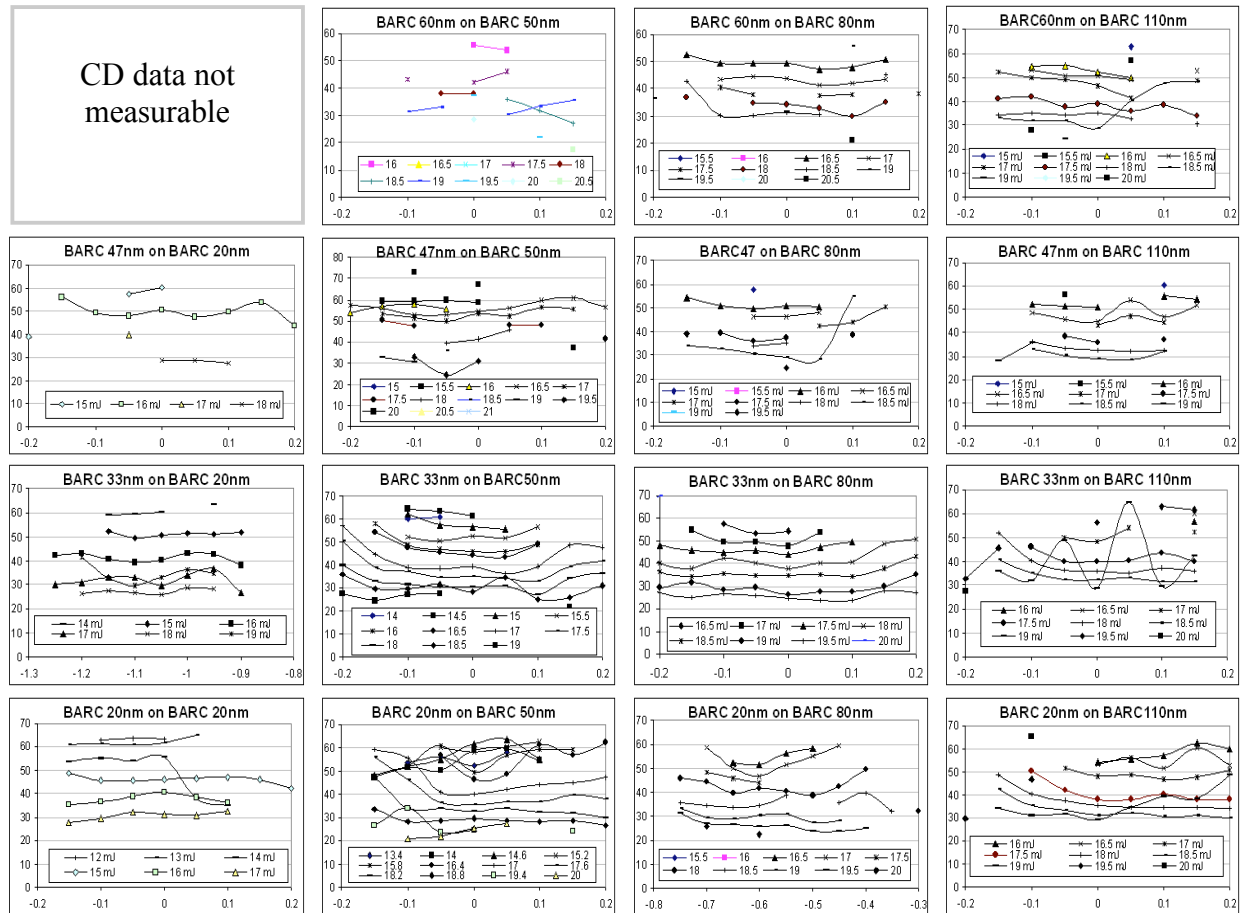


Figure 4. Measurement results for the 16 points. CD versus depth of focus at different exposure doses for dipole illumination, where the x dimension is defocus in microns and the y dimension is CD size in nm.

Oxide substrate

Figure 5 gives the simulation results of a BARC on an SiO₂ substrate, that is, a 740-nm layer of SiO₂ was inserted in between the BARC and silicon substrate shown in Figure 1. Solid curves are reflectivity and dotted curves are FE. Figure 5(a) is for a single-layer BARC system. The reflectivity is fairly low over the entire thickness range. In this case, only FE needs to be considered. Figure 5(b) is for the dual-layer BARC system. As with the previous case, ARC[®]145 and ARC[®]113 are used as the upper and lower layers with *k* values of 0.45 and 0.13, respectively. The thickness of the bottom layer is fixed at 29 nm. Four thickness points are chosen for the test as shown in the figure.

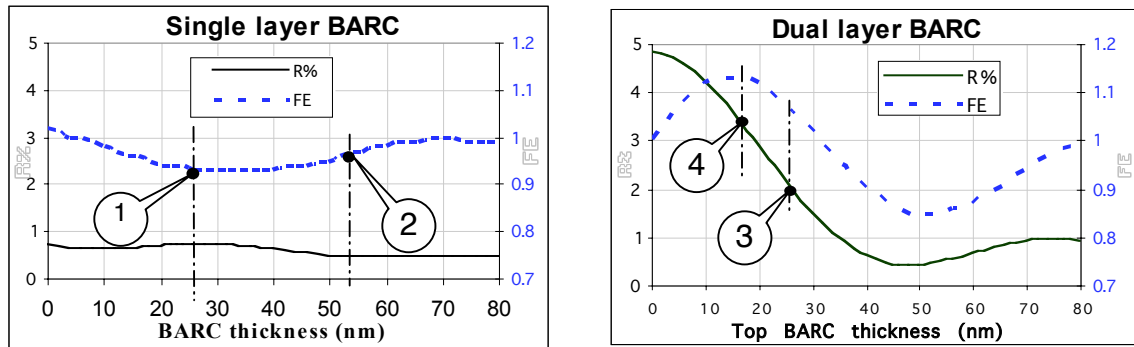


Figure 5. Simulation for oxide substrate reflection control; (a) single-layer BARC; (b) dual-layer BARC with bottom layer thickness fixed at 29 nm.

The CD measurement results are shown in Figure 6. The reflectivity of both the first and second points is very low, but the performance is very different. The second point has a much wider process window due to a higher FE value. The window is further opened by the increase of FE in the third and fourth points. Figure 7 is the defocus window for these four test points, limiting CD size deviation to within $\pm 10\%$ and exposure dose $\pm 5\%$. The first test point has no process window. The third test point has the widest window: 128 nm.

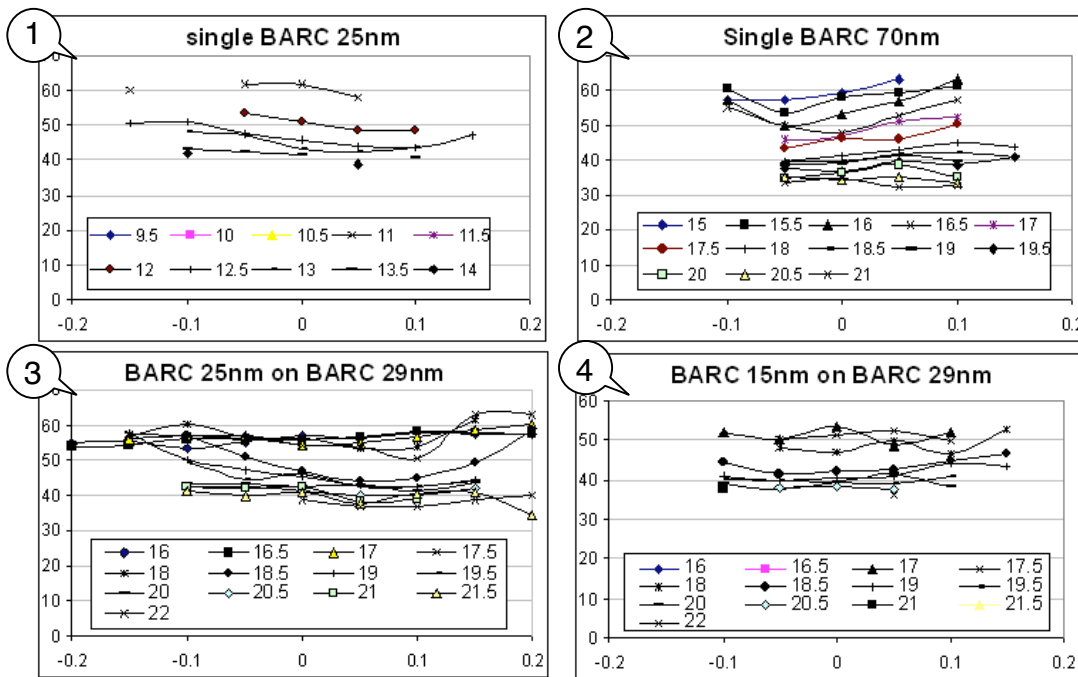


Figure 6. CD measurement results for the four test points.

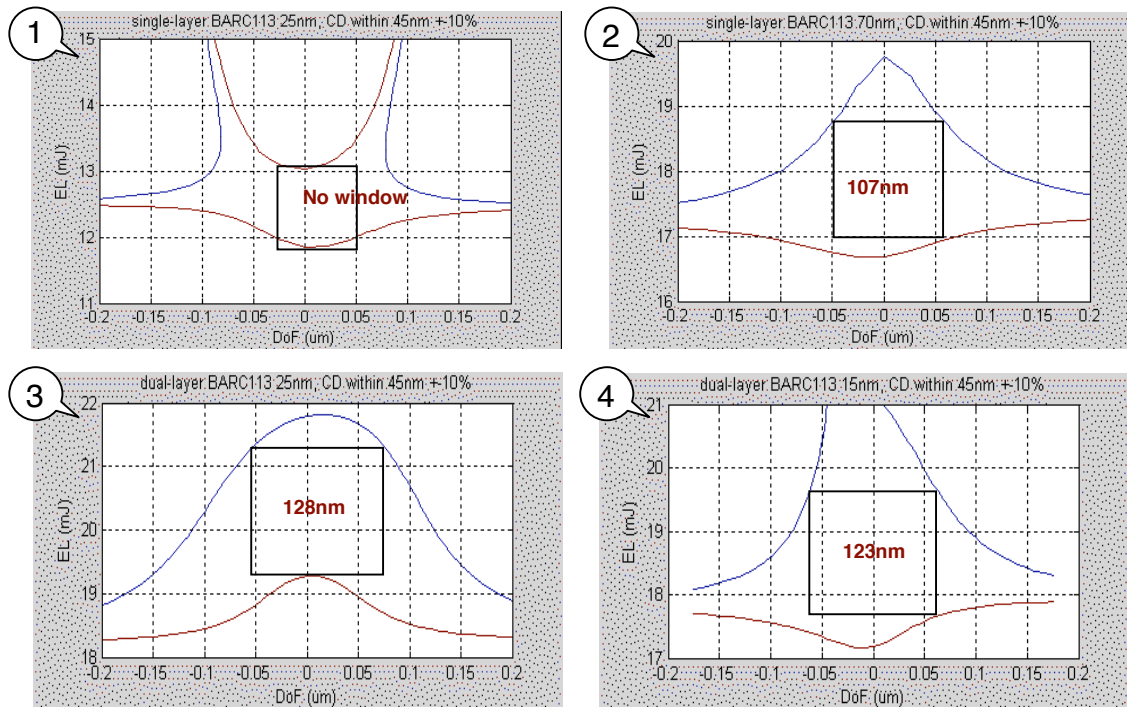


Figure 7. Defocus window for the four test points, with CD deviation within $\pm 10\%$ and exposure dose $\pm 5\%$.

4. DISCUSSION

Conventional BARC design aims to eliminate standing waves in the resist by minimizing reflectivity. However, the line profiles in Figure 2(f) do not show obvious standing wave signatures even though the standing wave amplitude is as high as 67%. All of the experimental results show that the minimum reflectivity does not give best performance. Thus the question is: What are the appropriate BARC design criteria? The answer is to have a good FE value in addition to low reflectivity. Generally FE should be a little bit higher than unity because of photoacid loss at the resist bottom due to its diffusion into the BARC layer. For this reason, BARC materials are often modified with some pH level or contain photoacid generator to control footing and undercut. Therefore FE as a design parameter can be used to compensate chemical footing or undercut.

The BARC design target should be obtaining the required FE with minimum reflectivity. A dual-layer BARC has an advantage for reaching this goal. When compared, the best single-layer BARC results (left picture of figure 2(c)) and the best dual-layer BARC results (third row, third column in Figure 4) have similar FE values. But the dual-BARC case has a much wider processing window due to its low reflectivity of 1%, compared to 2.5% for the single-layer BARC case. Another reason for lower reflectivity is to avoid potential pitch-dependent issues.

5. ACKNOWLEDGEMENTS

This work was supported by SEMATECH Resist Test Center personnel Andy Rudack, Dan Cochran, Cecilia Montgomery, Khurshid Anwar, Sandy Finkey, Paula Yergeau, and Scott Wright.

REFERENCES

1. Brewer, T., Carlson, R., and Arnold, J., "The Reduction of the Standing-Wave Effect in Positive Photoresists," *Journal of Applied Photographic Engineering*, vol. 7, no. 6, 184-186 (1981).

2. Guerrero, D.J., Smith, T., Kato, M., Kimura, S., and Enomoto, T., "Two-layer anti-reflection strategies for implant applications," *Proceedings of SPIE*, vol. 6153, 242-249 (2006).
3. He, L., Puligadda, R., Lowes, J., and Rich, M., "Bottom Anti-Reflective Coatings (BARCs) for 157-nm Lithography," *Proceedings of SPIE: Advances in Resist Technology and Processing XXI*, vol. 5376, 648-654 (2004).
4. Weimer, M., Wang, Y., Neef, C.J., Claypool, J., Edwards, K., and Zhu, Z., "Materials for and performance of multilayer lithographic schemes," *Proceedings of SPIE*, vol. 6519, 65192S-1 - 65192S-8 (2007).